Structural Engineering and Mechanics, Vol. 43, No. 6 (2012) 795-821
DOI: http://dx.doi.org/10.12989/sem.2012.43.6.795

Multiobjective size and topolgy optimization of dome structures

Talaslioglu Tugrul*

Department of Civil Engineering, Osmaniye Korkut Ata University, 8000, Osmaniye, Turkey

(Received November 15, 2011, Revised June 22, 2012, Accepted August 9, 2012)

Abstract. The size and topology of geometrically nonlinear dome structures are optimized thereby minimizing both its entire weight & joint (node) displacements and maximizing load-carrying capacity. Design constraints are implemented from provisions of American Petroleum Institute specification (API RP2A-LRFD). In accordance with the proposed design constraints, the member responses computed by use of arc-length technique as a nonlinear structural analysis method are checked at each load increment. Thus, a penalization process utilized for inclusion of unfeasible designations to genetic search is correspondingly neglected. In order to solve this complex design optimization problem with multiple objective functions, Non-dominated Sorting Genetic Algorithm II (NSGA II) approach is employed as a multi-objective optimization tool. Furthermore, the flexibility of proposed optimization is enhanced thereby integrating an automatic dome generating tool. Thus, it is possible to generate three distinct sphere-shaped dome configurations with varying topologies. It is demonstrated that the inclusion of brace (diagonal) members into the geometrical configuration of dome structure provides a weight-saving dome designation with higher load-carrying capacity. The proposed optimization approach is recommended for the design optimization of geometrically nonlinear dome structures.

Keywords: dome structure; geometrically nonlinear; NSGAII; API RP2A-LRFD

1. Introduction

The design of a dome structure, which is utilized to span large areas without an intermediate support, has been one of the challenging application problems in engineering optimization field (Saka 2007a, Kaveh 2010, Hasancebi 2009). The dome structures are generally constructed by use of tubular steel sections in a way of welding its steel members to each other. Therefore, they are lighter and cheaper compared to those constructed by use of ready profiles with different geometric cross-sections. But, both possibility of including slender members and welding process cause to increase the effect of bending moments on axial stiffness of the steel members (Saka 1998). Thus, dome structure can exhibit structural instability leading to a significant change in its structural configuration even when the static responses are well below a yield point of material. The optimal design of geometrically nonlinear steel structures were accomplished based on either using strain energy densities of its members for maximizing critical loads (Khot 1985, Kamat 1984, Sedaghati 2000, Levy 1988, 1994a, b) or design sensitivity information (Cardoso 1988, Choi 1987, Santos

*Corresponding author, Ph.D., E-mail: talaslioglu@cu.edu.tr, ttalaslioglu@osmaniye.edu.tr

1988, Ohsaki 2001, 2005, 2006). Recent optimization approaches performed for geometrically nonlinear steel structures have directly involved a robust nonlinear structural analysis method into their optimization procedures (Hrinda 2008). This nonlinear structural analysis has been also integrated with provisions of an available design specification (Saka 2007b, Carbas 2011, Kaveh 2011). In this regard, the member responses of the steel structure are computed where the determinant value of global rigidity matrix becomes to be positive. But, checking the strengths of its members computed at each incremental step of nonlinear structural analysis is neglected. Thus, the computing expense is correspondingly increased due to discarding the designations are resulted with a negative determinant of global rigidity matrix (Kannan 2009).

The other important task in the design optimization of geometrically nonlinear dome structures is the determination of the most appropriate one from several design criteria (entire weight, node displacement, load-carrying capacity etc.) conflicted to each other. In order to deal with this bottleneck, one of the reasonable approaches is to employ a multi-objective optimization algorithm for optimization-related computing procedure. Although a recent extended overview on the usage of multiple objectives for design optimization problems of structural engineering is presented in Reference Talaslioglu (2011), a study about multi-objective design optimization of geometrically nonlinear dome structures according to an available design specification is not found in the literature.

A general multi-objective optimization problem with N design (decision) variables is consisted m objective functions and J constraints. Its mathematical expression is given as

$$\min/\max F(x) = \{(f_1(x)), (f_2(x)), \ldots, (f_m(x))\}, \quad x \in DS \tag{1}$$

$$DS = \{x_n^L \le x_n \le x_n^U, \quad n = 1, 2, \ldots, N\} \tag{2}$$

$$SS = \{x : g_j(x) \le 0, \quad j = 1, 2, \ldots, J\} \tag{3}$$

A decision variable set defined in design variable space (DS) is represented by X bounded by upper and lower values, x_n^U and x_n^L. Thus, objective functions f and constrains $g_j(x)$ are accordingly computed in a solution space (SS).

At each run of an evolutionary optimization algorithm, a set of random solutions is obtained. Some of them are non-dominated solutions (none is better for all objectives) and referred as “pareto solution” defined in a concept named as domination (Srinivas 1995). Thus, the pareto solutions are used to form “pareto front” which determines bounds of non-dominated solutions.

The first multi-objectives optimization methods utilized gradient information derived from objective functions in order to compute the decision variables of continuous type (Talaslioglu 2011). However, these mathematical programming approaches easily failed when search space was concave and discontinuous. Although aggregating approaches such as weighted sum, game theory (Deb 2001a, Sunar 2001) were utilized as multi-objectives optimization methods, evolutionary based algorithms has been achieved to become the most attractive one (Talaslioglu 2011, Sepehri *et al.* 2012). The main feature of the evolutionary based multi-objective algorithms is their ability of either including or excluding the pareto solutions into optimization related computing procedure. One of the first evolutionary based multi-objective algorithms, named as Vector Evaluated Genetic Algorithm Schaffer (1984) did not utilized pareto solutions. In order to improve the computing capacity of the preliminary evolutionary based multi-objective algorithms, pareto solutions have been involved into solving mechanism of new multi-objective optimization procedures (Non-dominated Sorting Genetic Algorithm (NSGA) by Srinivas (1995), a Niched Pareto Genetic Algorithm (NPGA) by Horn (1994), a Multi-objective Genetic Algorithm (MOGA) by Fonseca (1993), and a Multi-objective Evolutionary Algorithm (MOEA) by Tanaka (1992)). Then, the improvement of their optimal results has been attained thereby i) enhancing their current optimization strategies, such as Non-dominated Sorting Genetic Algorithm II (NSGA II) (Deb (2001b, 2002), Improved Strength Pareto Evolutionary Algorithm II (SPEA II), Improved Pareto Envelope-Based Selection Algorithm (Region-Based Selection) II (PESA II), ii) adapting a competitive Search Technique, such as Adapting Scatter Search AbYSS (see Sunar (2001) for a further consideration of these optimization algorithms).

In this study, optimal size and topology of geometrically nonlinear dome structures is determined by minimizing both its entire weight and node displacements and maximizing its load-carrying capacity. The structural responses of dome structure are computed by using a software package ANSYS to run the computing procedure of arc-length method as a nonlinear structural analysis approach. The design constraints are implemented from provisions of API RP2A-LRFD. In the generation of optimal designations, the qualities of objective function values are evaluated according to the computing basis of NSGAII approach. The computing steps of proposed design optimization procedure are accordingly coded in MATLAB.

The organization of this study begins by a brief introduction to both multi-objectives optimization approaches and geometrically nonlinearity issue utilized in dome structure. Then, following the presentation of design constraints implemented from API RP2A-LRFD, an application example with two members is included to verify the member responses obtained by arc-length method. The computing steps of proposed design optimization approach are described in Chapter 4 by defining both design&optimization-related parameters and toolbox names according to codes in MATLAB scripts. The design results obtained are evaluated taking into account of a search methodology presented in Chapter 5 and summarized in Chapter 6. The last section is reserve for conclusion.

2. Design constraints defined according to provisions of API RP2A-LRFD specification

In this study, the size and topology optimization of the dome structures are carried out according to design constraints based on provisions of API RP2A-LRFD specification. For this purpose, the total weight of dome structure, f_1 and node displacements, f_2 are minimized whereas its carrying capacity, f_3 is maximized. It is noted that the member forces are utilized to define the carrying capacity of dome structure (see Eqs. (4)-(9)). Thus, the higher values of member forces indicate an increase in carrying capacity of dome structure. The member forces, f_3. The objective functions are is formulated as

$$f_1 = \sum_{k=1}^{m} (w*l)_k \quad (k = 1, \ldots, m) \tag{4}$$

$$f_2 = \min(d_{ij}) \quad (i = 1, \ldots, 12 \text{ and } j = 1, \ldots, n) \tag{5}$$

$$f_3 = \min(s_{ij}) \quad (i = 1, \ldots, 12 \text{ and } j = 1, \ldots, n) \tag{6}$$

Design constraints as

$$g_{Axial} = \begin{cases} Unity_{Axial} & : Unity_{Axial} \geq 1 \\ 0 & : Unity_{Axial} < 1 \end{cases} \quad (k = 1, \ldots, m) \tag{7}$$

$$g_{Bending} = \begin{cases} Unity_{Bending} & : Unity_{Bending} \geq 1 \\ 0 & : Unity_{Bending} < 1 \end{cases} \quad (k = 1, \ldots, m) \tag{8}$$

$$g_{CombinedBending} = \begin{cases} Unity_{CombinedBending} & : Unity_{CombinedBending} \geq 1 \\ 0 & : Unity_{CombinedBending} < 1 \end{cases} \quad (k = 1, \ldots, m) \tag{9}$$

$$g_{Shear} = \begin{cases} Unity_{Shear} & : Unity_{Shear} \geq 1 \\ 0 & : Unity_{Shear} < 1 \end{cases} \quad (k = 1, \ldots, m) \tag{10}$$

$$g_{AxialCompr\&BendingBuck} = \begin{cases} Unity_{AxialCompr\&BendingBuck} & : Unity_{AxialCompr\&BendingBuck} \geq 1 \\ 0 & : Unity_{AxialCompr\&BendingBuck} < 1 \end{cases} \quad (k = 1, \ldots, m) \tag{11}$$

$$g_{Torsion} = \begin{cases} Unity_{Torsion} & : Unity_{Torsion} \geq 1 \\ 0 & : Unity_{Torsion} < 1 \end{cases} \quad (k = 1, \ldots, m) \tag{12}$$

$$g_{AxialCompr\&BendingYield} = \begin{cases} Unity_{AxialCompr\&BendingYield} & : Unity_{AxialCompr\&BendingYield} \geq 1 \\ 0 & : Unity_{AxialCompr\&BendingYield} < 1 \end{cases} \quad (k = 1, \ldots, m) \tag{13}$$

Displacement constraint as,

$$g_{Disp} = \begin{cases} \dfrac{d_{ij}}{d_{\max}} & : d_{ij} \geq d_{\max} \\ 0 & : d_{ij} < d_{\max} \end{cases} \quad (i = 1, \ldots, 12 \text{ and } j = 1, \ldots, n) \tag{14}$$

The term W is computed depending on member length l and unit weight w assigned from a circular-shaped steel profile list. While d_{ij} is termed as node displacement corresponding to the related degree of freedom i and node j, the terms n and m indicate total numbers of node and dome member. Axial force of dome members (compression and tension) f_a, bending moment strength of dome member s f_{by} and f_{bz}, and shear strength of dome member s f_v in the constraints are limited by allowable nominal axial force (compression and tension) F_a and F_t, nominal shear strength F_v, Nominal Yield Strength F_y, Nominal Elastic and In-elastic Local Buckling Strength, F_{xe} and F_{xc}. Displacements of nodes are constrained by an upper limit $d_{\max}$. The proposed structural analysis of steel structures is performed to obtain the outputs (f_a, f_{by}, f_{bz} and f_v). The determination of nominal strengths $F_{a,}$ F_t, F_v, F_y, F_{xe} and F_{xc} according to provisions of API RP2A-LRFD specification is formulated in Appendix I.

3. Application of nonlinear structural analysis method, arc-length method to design example

ANSYS is employed to perform the computing procedures of arc-length method (see the governing equitation in Eq. (15) and chapter 15.3.6. arc-length method in ANSYS help for a further consideration).

$$[K_i^T]\{\Delta u_i\} - \Delta\lambda\{F^a\} = \{\lambda_n + \lambda_i\}\{F^a\} - \{F_i^{nr}\} = -\{R_i\} \tag{15}$$

A truss system which was used by Sedaghati (2000) (Fig. 1(a)) is devised in order to validate its responses obtained by ANSYS. *LINK1*-element assigned from ANSYS element database is used to represent truss member. A basic command list governed arc-length method are written in a file with an extension named "mac". The basic parameter values of these commands are taken as: *F* for convergence label, 0.0001 for convergence tolerance (see command *CNVTOL*), 400 for load step (see command *NSUBST*), 40 for maximum arc-length multiplier and 0.004 for minimum arc-length multiplier (see command *ARCLEN*). After the computation of nonlinear responses by arc-length method, it is observed that this truss system exhibits snap-through behavior (Fig. 1(b)). In Fig. 1(b), the variations on member force, stress and load factor with displacement are sketched. According to Fig. 1 the load, displacement and stress values set (200 lbs, 1.0567 inch, 1333 lbs/in^2) corresponding to the limit point obtained by Sedaghati (2000) is a good agreement with the set of (200 lbs, 1.052 in and 1330 lbs/in^2) obtained by ANSYS. It is noted that both force and stress values of truss members is increased to their maximum values 12999 lbs and 2002 lbs/in^2 although load factor that is computed using arc-length approach is decreased after passing a limit point corresponding to the displacement value (1.052 in) and load factor value (200 lbs).

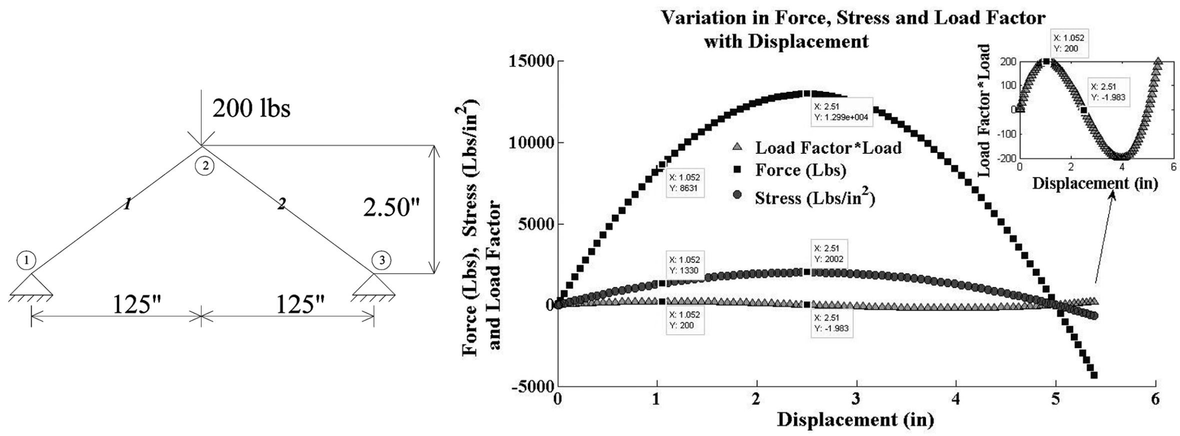

(a) (b)

Fig. 1 (a) A Truss structure with two-bars for verification example and (b) illustration of its snap-through behavior

4. Solving optimal design problem of geometrically nonlinear dome structure by NSGA II optimization algorithm

Sphere shapes are used to form the geometrical configuration of the dome structures. Both longitudinal-horizontal arched (chord) and diagonal members are utilized to construct the dome structure (see Fig. 2). Hence, three geometrical configurations are offered to generate the sphere-shaped dome structures using size and topology-related design variables (see Table 1). The size-related design variables Par_{DV} are represented by a steel profile database with 37 ready circular hollow cross-sections. Thus, the upper and lower limit of size-related design variables Par_{DVU} and Par_{DVL} are 37 and 1. The topology-related design variables are represented by longitudinal-horizontal division numbers Par_{LDN} and Par_{HDN} and used to determine longitudinal and horizontal arched members of dome structures located on semi sphere. The upper and lower limits of longitudinal and horizontal division numbers are Par_{LDNU} & Par_{LDNL} and Par_{HDNU} & Par_{HDNL}. In this regard, the sphere-shaped dome structure is generated by use of mathematical expression formulated by Eq. (16).

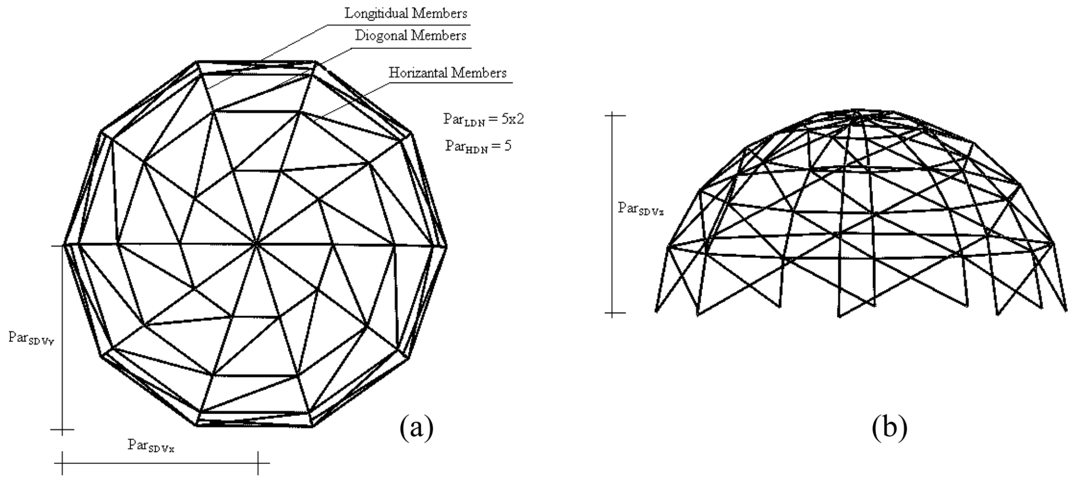

Fig. 2 (a) Top and (b) side view of sphere-shaped dome structure

Table 1 Three geometrical configurations used to arrangement of arched and diagonal members for sphere-shaped dome structures

	Geometrical Configuration 1	Geometrical Configuration 2	Geometrical Configuration 3
Cross-sectional Properties of Longitudinally Arched Members	Same	Different	Different
Cross-sectional Properties of Horizontally Arched Members	Different	Different	Different
Cross-sectional Properties of Diagonal Members	Not Included	Different	Not Included

```
FitnessFunction = @ObjElips;
numberOfVariables = 18;                                        % Number of decision variables
lb = [2 2 20 20 20 1  1  1  1  1  1  1  1  1  1  1  1  1];     % Lower bound
ub = [5 5 20 20 20 37 37 37 37 37 37 37 37 37 37 37 37 37];    % Upper bound

options = gaoptimset('Generations',100);
options.CreationFcn= @gacreationuniform ;
options.SelectionFcn= @selectionuniform ;
options.PopulationSize=50;
options.MutationFcn= {@mutationuniform, 0.50};
options.CrossoverFcn= {@crossoverheuristic,0.80};

Gamultiobj
        % Validate constraints and options
        gacommon
        % Call appropriate multi objective optimization solver
        gamultiobjsolve
                % Create initial state: population, Evaluate fitness functions
                GamultiobjMakeState
                        % Evaluate fitness function to get the number of objectives
                        feval(options.CreationFcn) (see ROUTINE1)
                        % Evaluate fitness function to get the number of objectives
                        Fcnvectorizer
                        % Get the rank and Distance measure of the population
                        rankAndDistance
```

ROUTINE1

1. Divide the applied loads (F^a) by into *n* load step
2. Assume $\left\{u_{i=0}\right\} = 0$
3. Compute tangent matrix $\left[K_i^T\right]$ and restoring load $\left\{F_i^{nr}\right\}$ from configuration $\left\{u_i\right\}$
4. Compute the incremental load factor ($\Delta\lambda$) depending on Δu_i and the proportional loading factor (λ) by an explicit spherical iteration method in a way of ensuring an orthogonallity condition that is offered by Forde & Stiemier (1987)
5. Check the convergence degree that controls the termination condition of iteration process using the resulted vector called as residual vector (R_i)
6. Compute the responses (element forces, stresses and node displacements) corresponding to the time step *n* and evaluate them according to provisions of API RP2A-LRFD specification, if convergence degree is satisfied.
7. Repeat steps 3 to 6 until any of design requirements API RP2A-LRFD specification (see Eqns. 7-13) is violated.
8. Save the entire weight of dome structure f_1, node displacements f_2 and element forces f_3 (see Eqns (4-6)).

ROUTINE 2

```
% Selection.
1. feval(options.SelectionFcn)
% Crossover
2. feval(options.MutationFcn)
% Evaluate fitness function
3. Fcnvectorizer
% Get the rank and av. Distance
4. rankAndDistance
% Calculate av. distance, spread
5. distanceAndSpread
```

```
                % Give the plot/output Functions
                gadsplot
                gaoutput
                while true
                % check to see if any stopping criteria have been met
                gamultiobjConverged
                stepgamultiobj
                        ROUTINE1 and ROUTINE 2
                Migration
                migrate
                % Output and plot functions
                gadsplot
                gaoutput
```

Fig. 3 A Pseudo code for NSGA II in conjunction with its toolbox names

$$\left.\begin{array}{l} x = Par_{SDVx}*\cos((\mathrm{pi}/2)*V)*\cos(\mathrm{pi}/U) \\ y = Par_{SDVy}*\cos((\mathrm{pi}/2)*V)*\sin(\mathrm{pi}/U) \\ z = Par_{SDVz}*\sin((\mathrm{pi}/2)*V) \end{array}\right\{ \begin{array}{l} U = 1/\mathrm{Par}_{\mathrm{LDN}},\ V = \mathrm{Par}_{\mathrm{LDN}} \\ \\ Par_{SDVx} = Par_{SDVy} = Par_{SDVz} \text{ for sphere shapes} \end{array} \tag{16}$$

The computing steps of the proposed optimization algorithm are presented by a pseudo code without including their arguments passing to other toolboxes (see MATLAB toolbox names in Fig. 3). Thus, the governing parameter values of NSGAII optimization algorithm are easily altered since they are coded in structure fields. It is noted, *BM3D*-element assigned from ANSYS element database is used to represent members of dome structure.

According to the pseudo code, the first step is the creation of fitness functions f_1, f_2 and f_3 (see ROUTINE1 defined by *FitnessFunction* in Fig. 3). For this purpose, these fitness functions are accordingly formulated for definition of a dome structure which is constructed by use of size, and topology-related design variables. Thus, the first individual of any population, x^0 and the upper-lower values of design variables (*lb* and *ub*) are formulated by Eqs. (17)-(19).

$$x^0 = \left[\underbrace{\mathrm{fix}(x_1^0), \mathrm{fix}(x_2^0)}_{Par_{LDN} \text{ and } Par_{HDN}} \quad \underbrace{x_3^0, x_4^0, x_5^0}_{Par_{SDVx},\ Par_{SDVy} \text{ and } Par_{SDVz}} \quad \underbrace{\mathrm{fix}(x_1^0), \mathrm{fix}(x_2^0)}_{Par_{DV}} \right] \begin{cases} \mathrm{Par_{ND}} = \mathrm{Par_{HDN}} & \text{for Geom. Comfig.1} \\ \mathrm{Par_{ND}} = 2*\mathrm{Par_{HDN}} + (\mathrm{Par_{HDN}} - 2) & \text{for Geom. Comfig.2} \\ \mathrm{Par_{ND}} = 2*\mathrm{Par_{HDN}} - 1 & \text{for Geom. Comfig.3} \end{cases} \tag{17}$$

$$lb = \left[\underbrace{Par_{LDNU}, Par_{HDNU}}_{Par_{LDN} \text{ and } Par_{HDN}} \quad \underbrace{Par_{SDVxU}, Par_{SDVyU}, Par_{SDVzU}}_{Par_{SDVx},\ Par_{SDVy} \text{ and } Par_{SDVz}} \quad \underbrace{Par_{DVU}, \ldots, Par_{DVU}}_{Par_{DV}} \right] \tag{18}$$

$$ub = \left[\underbrace{Par_{LDNL}, Par_{HDNL}}_{Par_{LDN} \text{ and } Par_{HDN}} \quad \underbrace{Par_{SDVxL}, Par_{SDVyL}}_{Par_{SDVx},\ Par_{SDVy} \text{ and } Par_{SDVz}} \quad \underbrace{Par_{DVL}, \ldots, Par_{DVL}}_{Par_{DV}} \right] \tag{19}$$

The maximum number of design variables (*numberOfVariables*), Par_{ND} are limited into 13 due to $Par_{HDNU} = 5$ for geometrical configuration 2 (see Eq. (17) and Fig. 3). The fitness values are computed by use of some numbers located in each individuals depending on two parameters Par_{LDN} and Par_{HDN}. It is noted that the proposed multi-objective design optimization procedure does not require any penalization process since checking process is terminated once the design constraints defined by provisions of API RP2A-LRFD specification is violated at any incremental stage of nonlinear structural analysis. The fundamental parameter values and genetic operator names are defined by making use of a structure field name named as *option*. Then, the first toolbox named as *Gamultiobj* is executed by use of these parameters. In this toolbox, firstly design constraints and parameters defined in *option* are checked against the violation of their pre-defined values. Then, the computing procedure of NSGA II algorithm begins by an execution of the toolbox *gamultiobjsolve* which calls two toolboxes named *GamultiobjMakeState* and *stepgamultiobj*. In fact, *GamultiobjMakeState* named ROUTINE2 is used to constitute the toolbox named *stepgamultiobj*. The toolbox named *gamultiobjsolve* calls *GamultiobjMakeState* in order to create the first initial population using *options.CreationFcn*, compute fitness functions (*fcnvectorizer*), rank them (*rankAndDistance*). Also, an execution of evolutionary genetic operators named selection, mutation and crossover is executed in the toolbox named *GamultiobjMakeState* (indicated by ROUTINE2 in Fig. 3). NSGA II toolbox is equipped with rich features allowing the output to both plot and save. The desired output and plots are executed in two toolbox named *gadsplot* and *gaoutput*. The main generation that is ended according to the value of parameter *options.Generations* begins to run (see *gamultiobjConverged* for further information about the other termination options). Then, the toolbox named *stepgamultiobj* is employed to execute three evolutionary operators, selection, mutation and crossover which are defined by ROUTINE 1. The desired output is both saved and plotted by *gadsplot* and *gaoutput* following the activation of migration process.

5. Search methodology for evaluation of obtained results

The genetic search carried out by NSGAII algorithm is managed by probabilistic transition rules. Therefore, the computing complexity arisen from the number of interacted genetic parameters is high. However, the difficulty in determining an appropriate genetic parameter set is relatively low due to limiting the application area to the design optimization of geometrically nonlinear dome structures in structural engineering field. In this regard, four combination sets contained different parameter values of crossover and mutation operators are devised in associated with lower and higher population size. Thus, total eight parameter sets are considered to determine the best one allowing to an increase in the computing performance of NSGAII algorithm. Although the convergence degrees of optimal designations are utilized to assess the computing performance of any optimization approach with a single-objective function, it is not sufficient for multi-objective optimization approaches due to usage of multiple objective functions at same time. In this regard, different quality measuring metrics have been developed to evaluate the optimality quality of designations generated by any multi-objective optimization approach (Zhou and *et al.* 2011). In this study, well-known three quality indicators named spread, average distance and hyper-volume are utilized along with a statistical test procedure carried out in a certain level of confidence. Whereas the computing procedures of spread and average distances are already coded in current toolboxes, named *rankAndDistance.m, distancecrowding.m*, the code scripts of hyper-volume is externally included (see web page presented in Reference (12)]). In order to increase the consistency in assessing the values of these quality indicators, 100 different runs of proposed design approach are performed. While higher values of hyper-volume indicate a large coverage of non-dominated solutions in a solution space, a lower spread and average distance values are expected for a better and uniform distribution among non-dominated solutions. Furthermore, lower spread and average distance values indicate to locate non-dominated solutions in uniformly different position of solution space. Hence, if a probability value outcome from performing the statistical test procedure satisfies a user defined significance level, then it is said that current genetic parameter set is acceptable. Considering the average values of these quality indicators, the parameter sets corresponding to the lower spread and average distance and higher hyper-volume values are determined as the best parameter set.

5.1 Details of statistical test procedure

The computing procedures of the statistical analysis are performed in MATLAB. The spread and average distance values of each execution are stored. Then, the average values of these spread and average distance values are checked about whether to exhibit a normal distribution thereby employing the lillie test. If those values do not shown a normal distribution, a kruskal-wallis test method is utilized to compare these average spread and average distance values. Furthermore, in order to accomplish a more explicit comparison among them, a comparison of pairs is made using a post hoc 5% hsd-test (also known as Tukey-Kramer test) (see function “multicompare” in MATLAB Statistical Toolbox). Basically, this function returns a matrix of pair wise comparison results with information about which pairs of distributions are significantly different.

6. Results and discussion

A dome structure, which has an elasticity module of 205 kN/mm^2, a diameter of 20 m and an upper limit for node displacements taken as 28 mm, (see further details in Kaveh 2011) is devised as a design example. The design of this dome structure is optimized by use of 37 ready circular hollow cross-section properties (see Carbas 2011). The best parameter sets and dome configurations are determined using the values of three quality indicators. Furthermore, it is also proposed to highlight the requirement of using the multi-objective optimization approach for geometrically nonlinear dome structures. Therefore, this section is divided into two sub-sections, each of which contains a corresponding summarization of obtained results.

Table 2 Design variable and parameters governed the proposed optimal design approach

Parameter or Design Variable Names	Parameter and Design Variable Values							
Genetic Operator Parameter Names	Genetic Operator Parameter Combination No (GPCN)							
	1	2	3	4	5	6	7	8
options. Generations	100	100	100	100	100	100	100	100
options.PopulationSize	50	50	50	50	100	100	100	100
options.MutationFcn= {@mutationuniform,}	0.50	0.20	0.50	0.20	0.50	0.20	0.50	0.20
options.CrossoverFcn= {@crossoverheuristic,}	0.80	0.80	0.40	0.40	0.80	0.80	0.40	0.40
Design Variable Names	Design Variable Values							
Size Related Design Variables								
Par_{DV}	$Par_{DVL}=1 < <Par_{DVU}=37$							
Shape Related Design Variables								
Par_{SDVx}	$Par_{SDVxL}=19^m < <Par_{SDVxU}=21^m$				$Par_{SDVxL}=Par_{SDVxU}=20^m$			
Par_{SDVy}	$Par_{SDVyL}=19^m < <Par_{SDVyU}=21^m$				$Par_{SDVyL}=Par_{SDVyU}=20^m$			
Par_{SDVz}	$Par_{SDVzL}=19^m < <Par_{SDVzU}=21^m$				$Par_{SDVzL}=Par_{SDVzU}=20^m$			
Topology Related Design Variables								
Par_{LDN}	$Par_{LDNL} = 2 < <Par_{LDNU} = 5$							
Par_{HDN}	$Par_{HDNL} = 2 < <Par_{HDNU} = 5$							
Structural Analysis Related Parameter Names	Structural Analysis Related Parameter Values							
Convergence Tolerance (see com. CNVTOL)	0.00001							
Load step (see com.NSUBST)	500							
Arc-length mult. (see ARCLEN)	50							

6.1 Assessment of proposed parameter sets and determination of better geometrical configuration

In order to investigate the impact of genetic parameters on optimality quality of designations obtained, total eight genetic parameter combination sets (GPCN1-GPCN8) are proposed. In fact, these genetic parameter sets are obtained by combining higher-lower mutation rates (0.5-0.2) and crossover rates (0.8-0.4) with higher-lower population size (100-50) (see Table 2).

These proposed genetic parameter sets are applied for design optimization of a dome structure with $Par_{LDN} = Par_{LDN} = 2$, $Par_{LDN} = Par_{LDN} = 5$ and $Par_{LDN} = varying$, $Par_{LDN} = varying$. Thus, a variation in member number of dome structure is also taken into account for evaluation of genetic

Table 3 Pair wise comparison of spread values for sphere shaped geometrical configuration1 with GPCN1-GPCN8 come from the post-hoc testing named "multicompare"

GPCN	GPCN	Lower Bound	Average of Lower Bound and Upper Bound	Upper Bound
1	2	-154,01	-54,96	44,09
1	3	-180,11	-81,06	17,99
1	4	-177,29	-78,24	20,81
1	5	-205,57	-106,52	-7,47
1	6	-154,43	-55,38	43,67
1	7	-106,09	-7,04	92,01
1	8	-151,05	-52,00	47,05
2	3	-125,15	-26,10	72,95
2	4	-122,33	-23,28	75,77
2	5	-150,61	-51,56	47,49
2	6	-99,47	-0,42	98,63
2	7	-51,13	47,92	146,97
2	8	-96,09	2,96	102,01
3	4	-96,23	2,82	101,87
3	5	-124,51	-25,46	73,59
3	6	-73,37	25,68	124,73
3	7	-25,03	74,02	173,07
3	8	-69,99	29,06	128,11
4	5	-127,33	-28,28	70,77
4	6	-76,19	22,86	121,91
4	7	-27,85	71,20	170,25
4	8	-72,81	26,24	125,29
5	6	-47,91	51,14	150,19
5	7	0,43	99,48	198,53
5	8	-44,53	54,52	153,57
6	7	-50,71	48,34	147,39
6	8	-95,67	3,38	102,43

Table 4 A statistical assessment of spread, average distance and hyper-volume for proposed sphere-shaped geometrical configurations (Par_{LDN}=2, Par_{HDN}=2)

Geometrical Configuration	GPCN	Spread				Average Distance				Hyper Volume			
		max	min	average	Statistical significance	max	min	average	Statistical significance	max	min	average	Statistical significance
Sphere-shaped Geometrical Configuration 1	1	0.079	0.021	0.057	0.01592579	0.7936	0.2017	0.4805	0.01719158	0.3998	0.1013	0.2751	0.01605552
	2	0.095	0.020	0.063		0.9366	0.2018	0.5308		0.2497	0.1024	0.1790	
	3	0.089	0.021	0.058		0.8913	0.2087	0.5626		0.2999	0.1029	0.2203	
	4	0.084	0.020	0.060		0.8476	0.2192	0.5200		0.3457	0.1028	0.2407	
	5	0.090	0.020	0.060		0.8958	0.2193	0.5735		0.2990	0.1005	0.2199	
	6	0.084	0.021	0.058		0.8496	0.2003	0.5175		0.3477	0.1016	0.2445	
	7	0.075	0.021	0.051		0.7498	0.2047	0.4402		0.4477	0.1003	0.2827	
	8	0.080	0.020	0.056		0.7991	0.2082	0.5182		0.3964	0.1115	0.2743	
Sphere-shaped Geometrical Configuration 2	1	0.070	0.021	0.047	0.01487559	0.6990	0.2001	0.4712	0.00844113	0.4987	0.1017	0.3309	0.00416201
	2	0.085	0.021	0.057		0.8314	0.2122	0.5454		0.3482	0.1051	0.2422	
	3	0.075	0.023	0.049		0.7413	0.2038	0.4432		0.4480	0.1054	0.3046	
	4	0.079	0.021	0.048		0.7908	0.2358	0.5271		0.3986	0.1074	0.2749	
	5	0.079	0.020	0.053		0.7933	0.2005	0.5154		0.3972	0.1055	0.2678	
	6	0.065	0.020	0.044		0.8461	0.2015	0.5405		0.5398	0.1223	0.3612	
	7	0.070	0.021	0.049		0.6868	0.2035	0.4359		0.4965	0.1078	0.3167	
	8	0.074	0.020	0.051		0.7449	0.2033	0.4844		0.4444	0.1233	0.3052	
Sphere-shaped Geometrical Configuration 3	1	0.075	0.021	0.050	0.01324721	0.7414	0.2049	0.4729	0.00980036	0.3957	0.1016	0.2573	0.01841320
	2	0.085	0.021	0.056		0.8438	0.2001	0.5159		0.2495	0.1006	0.1793	
	3	0.090	0.020	0.058		0.8772	0.2038	0.5450		0.2991	0.1012	0.2135	
	4	0.080	0.021	0.055		0.7969	0.2157	0.5036		0.3482	0.1068	0.2391	
	5	0.079	0.021	0.055		0.7942	0.2056	0.4728		0.2996	0.1002	0.2086	
	6	0.085	0.023	0.059		0.8426	0.2157	0.4939		0.3485	0.1056	0.2416	
	7	0.070	0.021	0.048		0.6996	0.2151	0.4484		0.4481	0.1237	0.2969	
	8	0.075	0.021	0.053		0.7413	0.2001	0.4449		0.3977	0.1001	0.2488	

Table 5 A statistical assessment of spread, average distance and hyper-volume for proposed sphere-shaped geometrical configurations (Par_{LDN}=5. Par_{HDN}=5)

Geometrical Configuration	GPCN	Spread				Average Distance				Hyper Volume			
		max	min	average	Statistical significance	max	min	average	Statistical significance	max	min	average	Statistical significance
Sphere-shaped Geometrical Configuration 1	1	0.070	0.020	0.051	0.00411948	0.8455	0.2020	0.5144	0.00896022	0.3491	0.1008	0.2483	0.00831001
	2	0.085	0.022	0.058		0.6996	0.2037	0.4546		0.4988	0.1127	0.3443	
	3	0.080	0.021	0.055		0.7940	0.2204	0.4865		0.3992	0.1169	0.2758	
	4	0.075	0.020	0.050		0.7439	0.2030	0.4422		0.4468	0.1044	0.3044	
	5	0.079	0.022	0.056		0.7959	0.2002	0.4933		0.3993	0.1065	0.2569	
	6	0.069	0.020	0.047		0.6971	0.2053	0.4580		0.4970	0.1020	0.3323	
	7	0.074	0.021	0.051		0.7369	0.2079	0.4546		0.4459	0.1032	0.2864	
	8	0.065	0.022	0.046		0.6495	0.2004	0.4363		0.5391	0.1170	0.3427	
Sphere-shaped Geometrical Configuration 2	1	0.070	0.020	0.049	0.01692922	0.6941	0.2027	0.4417	0.01472192	0.4986	0.1064	0.3395	0.01112704
	2	0.065	0.020	0.043		0.6453	0.2043	0.4541		0.5450	0.1020	0.3587	
	3	0.075	0.020	0.050		0.7435	0.2005	0.4465		0.4498	0.1087	0.2941	
	4	0.058	0.020	0.041		0.5998	0.2024	0.3980		0.5939	0.1023	0.3762	
	5	0.065	0.021	0.046		0.6490	0.2016	0.4186		0.5461	0.1068	0.3643	
	6	0.060	0.021	0.042		0.5993	0.2090	0.4076		0.5976	0.1196	0.3954	
	7	0.070	0.020	0.046		0.6968	0.2064	0.4554		0.4989	0.1089	0.3043	
	8	0.055	0.021	0.040		0.5487	0.2005	0.3701		0.6484	0.1507	0.4280	
Sphere-shaped Geometrical Configuration 3	1	0.080	0.022	0.053	0.00994541	0.7820	0.2181	0.4964	0.00686949	0.3969	0.1045	0.2741	0.01055673
	2	0.064	0.020	0.045		0.6469	0.2002	0.4142		0.5497	0.1026	0.3648	
	3	0.069	0.021	0.046		0.6971	0.2039	0.4640		0.4978	0.1089	0.3344	
	4	0.074	0.020	0.051		0.4991	0.2095	0.3354		0.4452	0.1061	0.3062	
	5	0.075	0.021	0.051		0.7406	0.2001	0.4739		0.4427	0.1098	0.2853	
	6	0.065	0.020	0.045		0.6490	0.2052	0.4172		0.5462	0.1186	0.3393	
	7	0.070	0.022	0.049		0.6929	0.2061	0.4526		0.4994	0.1136	0.3285	
	8	0.060	0.020	0.041		0.5997	0.2018	0.3801		0.5904	0.1122	0.3712	

Table 6 A statistical assessment of spread, average distance and hyper-volume for proposed sphere-shaped geometrical configurations (Varying Topology)

Geometrical Configuration	GPCN	Spread				Average Distance				Hyper Volume			
		max	min	average	Statistical significance	max	min	average	Statistical significance	max	min	average	Statistical significance
Sphere-shaped Geometrical Configuration 1	1	0.060	0.020	0.041	0.00591774	0.7479	0.2037	0.4547	0.00230717	0.4499	0.1007	0.2917	0.00226123
	2	0.075	0.022	0.048		0.5867	0.2003	0.3864		0.5971	0.1058	0.4087	
	3	0.070	0.020	0.049		0.6967	0.2101	0.4480		0.4977	0.1214	0.3315	
	4	0.065	0.020	0.047		0.6496	0.2009	0.4457		0.5479	0.1017	0.3496	
	5	0.070	0.021	0.050		0.6984	0.2036	0.4171		0.4983	0.1200	0.3160	
	6	0.060	0.020	0.041		0.5948	0.2017	0.4028		0.5913	0.1092	0.3895	
	7	0.065	0.020	0.046		0.6461	0.2011	0.4138		0.5458	0.1232	0.3641	
	8	0.055	0.021	0.039		0.5485	0.2164	0.3872		0.6494	0.1176	0.4439	
Sphere-shaped Geometrical Configuration 2	1	0.060	0.020	0.042	0.01788833	0.5941	0.2056	0.3851	0.00507919	0.5995	0.1083	0.3857	0.00453963
	2	0.055	0.020	0.038		0.5499	0.2045	0.3609		0.6499	0.1450	0.4258	
	3	0.065	0.020	0.044		0.6497	0.2014	0.4395		0.5486	0.1273	0.3733	
	4	0.049	0.020	0.036		0.4999	0.2023	0.3580		0.6982	0.1104	0.4500	
	5	0.055	0.021	0.041		0.5494	0.2071	0.3663		0.6466	0.1497	0.4384	
	6	0.050	0.020	0.036		0.4998	0.2010	0.3441		0.6909	0.1192	0.4657	
	7	0.060	0.021	0.042		0.5944	0.2012	0.4058		0.5947	0.1048	0.4080	
	8	0.045	0.020	0.033		0.4481	0.2136	0.3390		0.7481	0.1293	0.5059	
Sphere-shaped Geometrical Configuration 3	1	0.070	0.020	0.047	0.00139300	0.6941	0.2013	0.4798	0.00149026	0.4896	0.1035	0.3213	0.00198096
	2	0.054	0.021	0.038		0.5485	0.2023	0.3711		0.6455	0.1140	0.4264	
	3	0.060	0.020	0.041		0.5985	0.2011	0.4173		0.5942	0.1184	0.3932	
	4	0.064	0.022	0.045		0.6498	0.2012	0.4338		0.5401	0.1009	0.3442	
	5	0.065	0.021	0.043		0.6477	0.2085	0.4037		0.5498	0.1078	0.3693	
	6	0.055	0.020	0.039		0.5402	0.2038	0.3823		0.5360	0.1156	0.3519	
	7	0.060	0.022	0.043		0.5940	0.2004	0.3901		0.5941	0.1280	0.3867	
	8	0.049	0.020	0.036		0.4973	0.2048	0.3397		0.6960	0.1908	0.4618	

Kruskal-Wallis ANOVA Table

Source	SS	df	MS	Chi-sq	Prob>Chi-sq
Groups	920495.9	7	131499.4	17.24	0.0159
Error	41746104.1	792	52709.7		
Total	42666600	799			

(a)

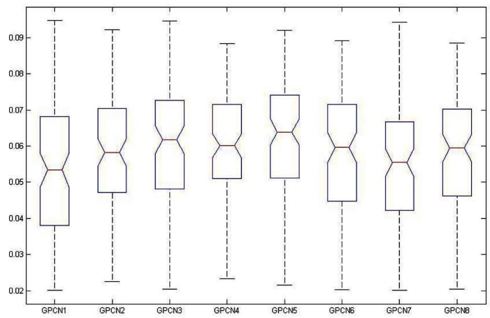

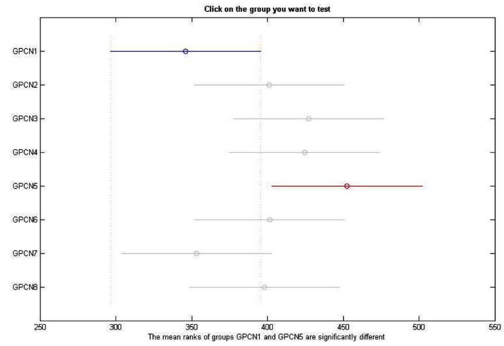

(b) (c)

Fig. 4 Kruskal-wallis test results for spread values for sphere-shaped geometrical configuration1 with GPCN1-GPCN8 for fixed topology (see Table 4 and Post-hoc Test named “multicompare” in MATLAB’ help)

parameter sets. The results obtained are summarized in Tables 4-6. According to statistical significance values listed in Tables 4-6, it is said that current genetic parameter seta are acceptable due to their lower values ($P < 0.5$). Furthermore, in order to highlight the statistical testing procedure, a visualization of statistical results obtained from MATLAB execution for design optimization of sphere-shaped geometrical configuration is presented for spread value in Figs. 4(a)-(c) (see cells corresponding to statistical significance value = 0.015925 in Table 4).

Considering Table 4, the success of GPCN1 is higher for a decrease in population size due to lower spread and average distance values (0.057-0.047-0.050 and 0.4805-0.4712-0.4729) and higher hyper-volume values (0.2751-0.3309-0.2573). However, an increase in population size is resulted with a success of GPCN7 due to lower spread and average distance values (0.051-0.048 and 0.4402-0.4484) and higher hyper-volume values (0.2827-0.2969) for geometrical configuration 1 and 3. Inclusion of diagonal members into geometrical configurations (see properties of geometrical configuration 2 in Table 1) causes to a decrease in mutation rate and an increase in crossover rate. Thus, the most success of genetic search is increased by use of GPCN6 along with geometrical configuration 2 due to lower spread and average distance value, 0.044 and 0.5405 and higher hyper-volume value 0.3612.

Taking into account of Table 5, an increase in the member number is resulted with the success of GPCN2 and GPCN4 for the decreased population size. The increase in population size causes to a decrease in mutation and crossover rates. Thus, lower spread and average distance values (0.046-0.040-0.041) and (0.4363-0.3701-0.3801) and higher hyper-volume values (0.3427-0.4280-0.3712) for three geometrical configurations 1-3. It is clear that geometrical configuration included diagonal members achieves to obtain the lowest spread and average values 0.40 and 0.3701 and highest hyper-volume value 0.4280.

The execution the proposed design approach for varying topology (Par_{LDN} = *varying*,

$Par_{LDN} = varying$) is resulted with similar results obtained by use of $Par_{LDN} = Par_{LDN} = 2$, $Par_{LDN} = Par_{LDN} = 5$ (see Table 6). Considering Table 6, the contribution of GPCN2 and GPCN4 along with decreased population size to the genetic search is higher than the other GPCN's due to lower spread and average distance values (0.041-0.036-0.038) and (0.3864-0.3580-0.3711) and higher hyper-volume values (0.3496-0.4500-0.4264). However, the success of GPCN8 is highest for increased population size due to lowest spread and average distance values (0.0330 and 0.3390) and highest hyper-volume value 0.5059.

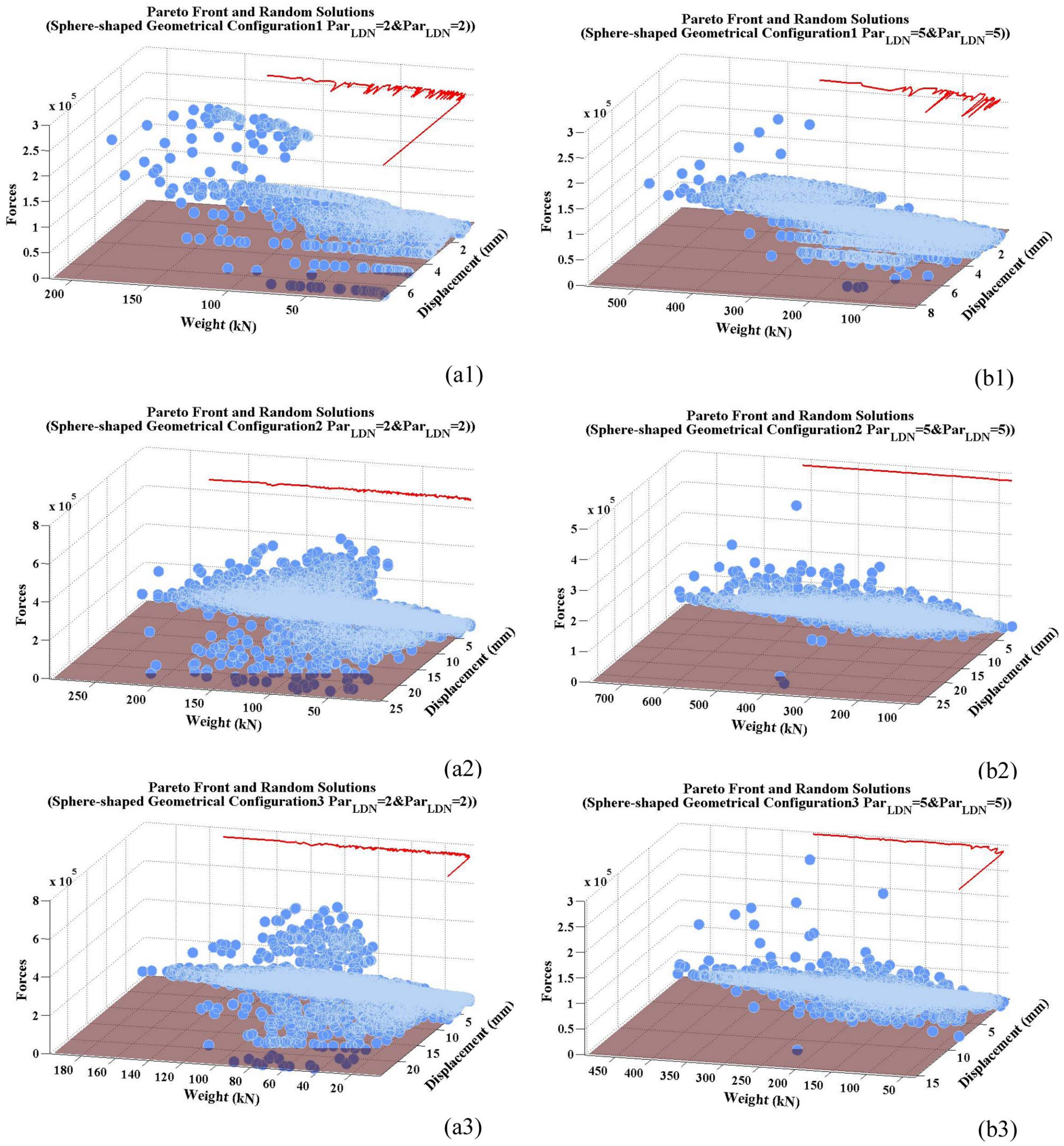

Fig. 5 Pareto fronts and random solutions sphere-shaped geometrical configurations with fixed topology-related design variables Par_{LDN}=2& Par_{HDN}=2 (a1-a3) and Par_{LDN}=5& Par_{HDN}=5 (b1-b3)

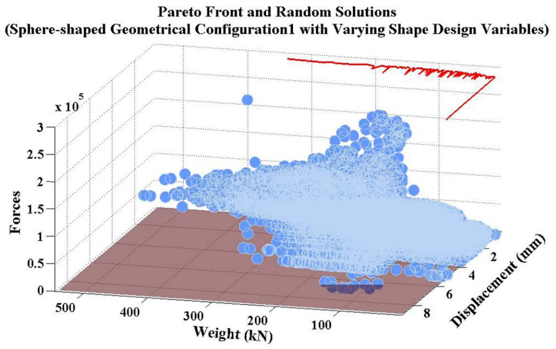

(a1)

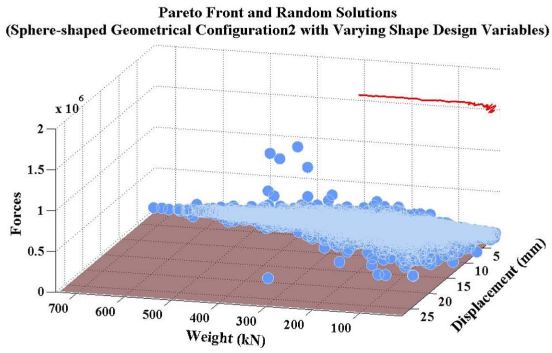

(a2)

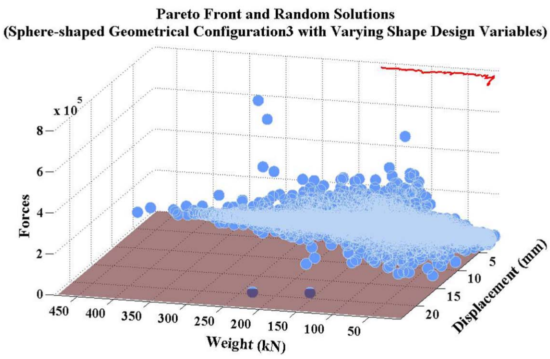

(a3)

Fig. 6 Pareto fronts and random solutions sphere-shaped geometrical configurations with varying topology-related design variables

6.2 Evaluation of relation between conflicted objective functions

In order to indicate the load-carrying capacity of dome structure, its member forces are utilized. Considering the literature for similar studies, usage of member forces as an indicator for load-carrying capacity of dome structure is firstly attempted in this study. In this regard, the relation between conflicted three objective functions, entire weight, node displacements and member forces is laid down. The forms of the pareto fronts obtained by use of three size and topology-related design variables ($Par_{LDN} = Par_{LDN} = 2$, $Par_{LDN} = Par_{LDN} = 5$ and $Par_{LDN} = varying, Par_{LDN} = varying$) are presented for each of three geometrical configurations (see red lines located on top of Figs. 5-6). In order to clarify the load-carrying capacity of dome structure obtained by use of different geometrical configurations, an external joint load taken as 1000 kN is also presented by a red surface. If the maximum member forces corresponding to a designation that satisfies the design constraints based on provisions of API RP2A-LRFD are higher than the external joint load value, then the corresponding maximum member force is utilized to indicate the load-carrying capacity of dome structure. In general, the load-carrying capacity of dome structures corresponding to random solutions obtained is higher than external joint load value (see Figs. 5-6). Furthermore, some extreme designations chosen from random solutions presented in Figs. 5-6 are both visualized for

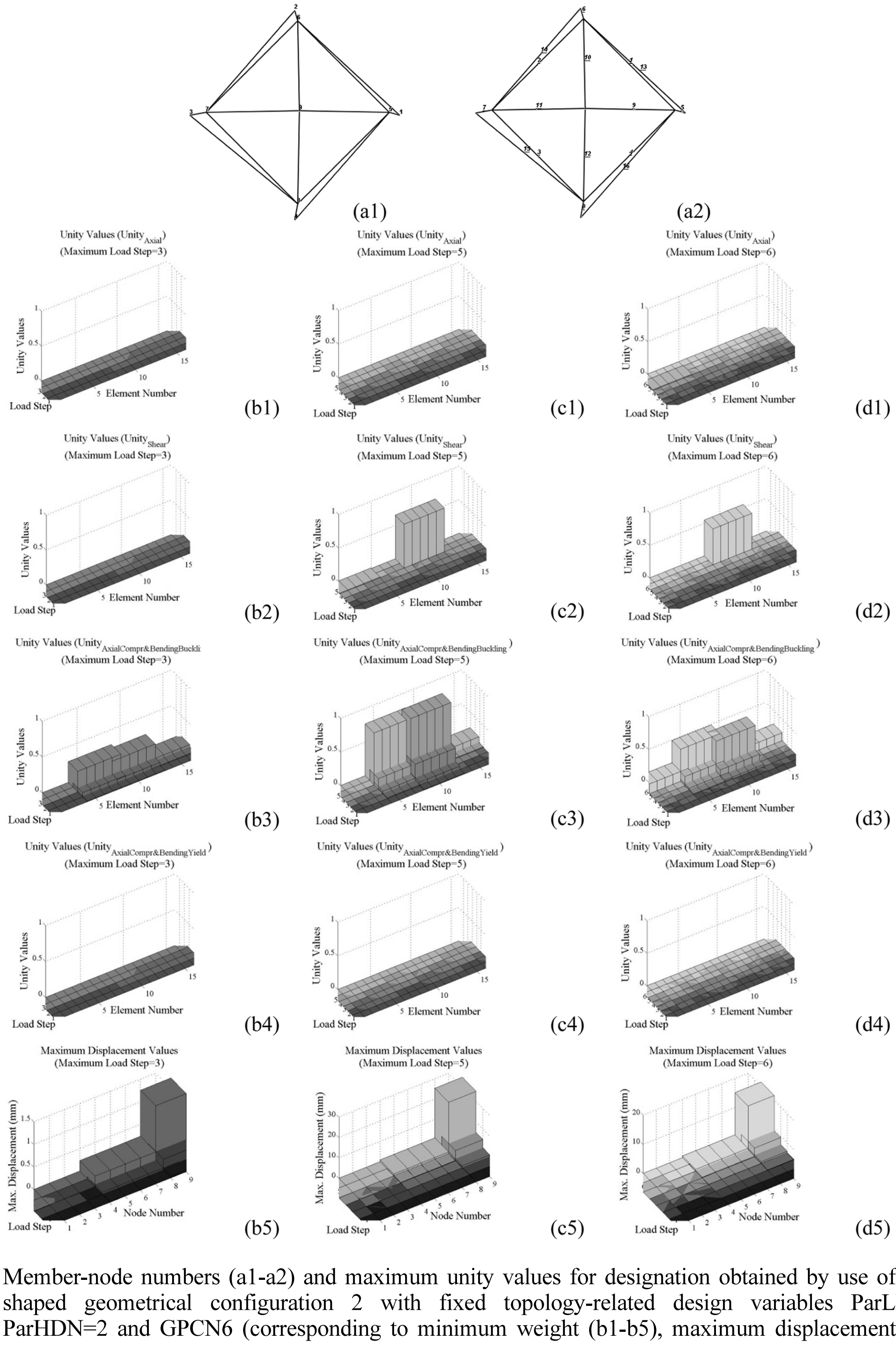

Fig. 7 Member-node numbers (a1-a2) and maximum unity values for designation obtained by use of sphere-shaped geometrical configuration 2 with fixed topology-related design variables ParLDN=2& ParHDN=2 and GPCN6 (corresponding to minimum weight (b1-b5), maximum displacement (c1-c5) and maximum force (d1-d5))

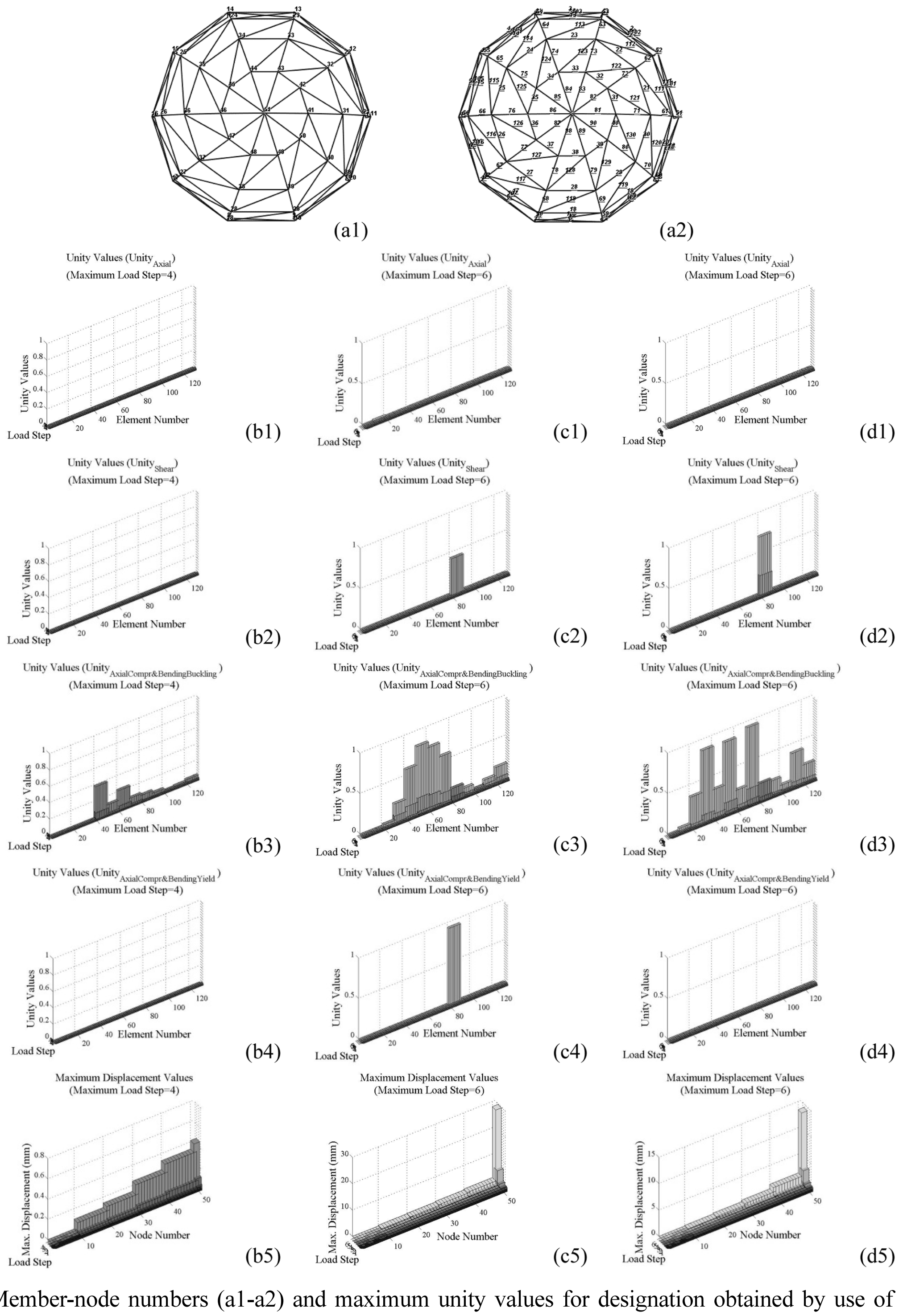

Fig. 8 Member-node numbers (a1-a2) and maximum unity values for designation obtained by use of sphere-shaped geometrical configuration 2 with fixed topology-related design variables ParLDN=5& ParHDN=5 and GPCN8 (corresponding to minimum weight (b1-b5), maximum displacement (c1-c5) and maximum force (d1-d5))

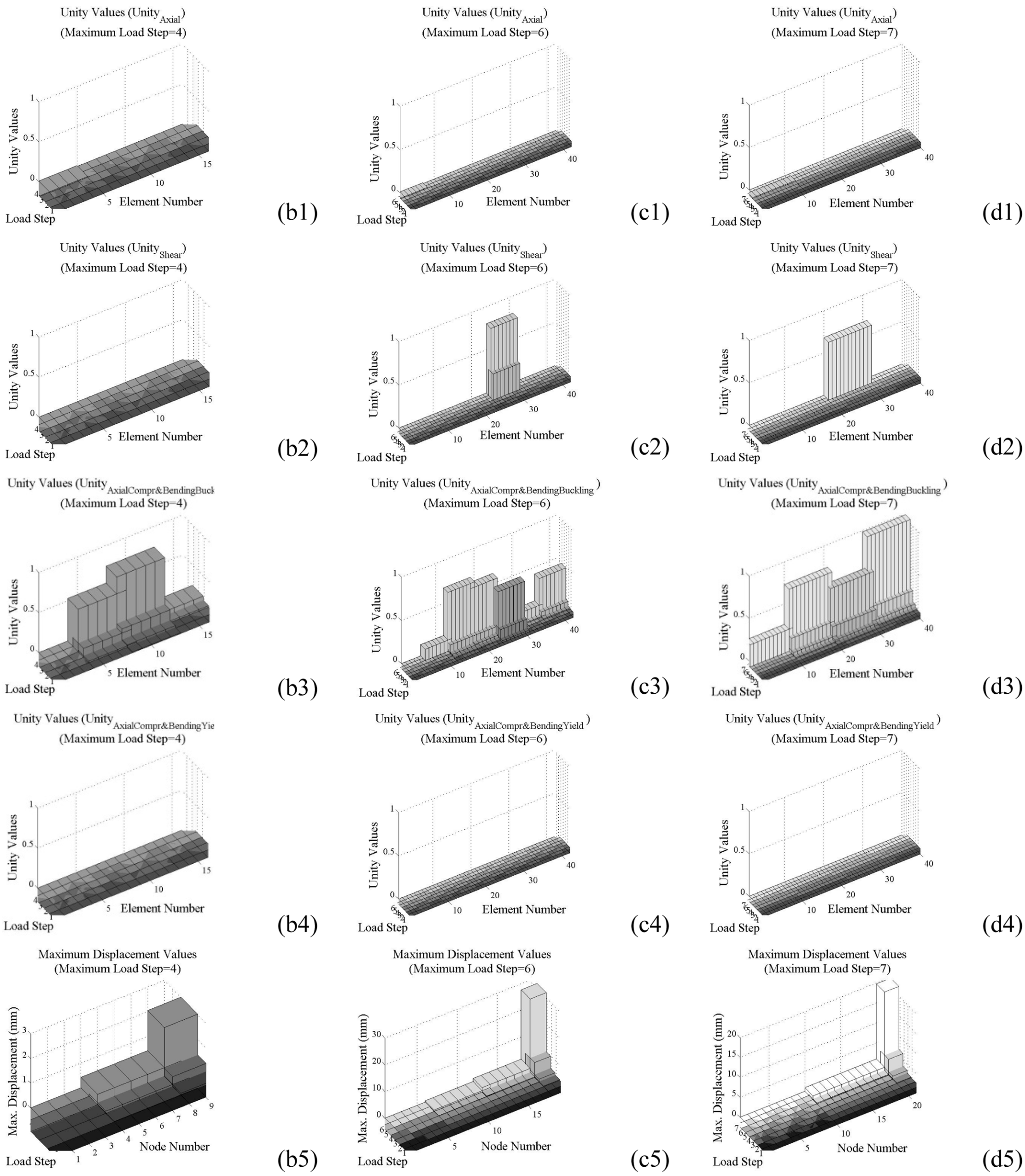

Fig. 9 Maximum unity values for designation obtained by use of sphere-shaped geometrical configuration 2 with varying topology-related design variables (corresponding to minimum weight (b1-b5), maximum displacement (c1-c5) and maximum force (d1-d5))

their design constraints at each load steps (see Figs. 7-9) and tabulated to report their objective function values along with design variables (see Tables 7-9).

Considering Tables 7-9, it is obvious that a decrease in the topology related design variables leads

Table 7 Values of size, shape-related design variable corresponding to designations with minimum weight, maximum displacement and maximum force obtained by use sphere-shaped geometrical configuration2 and GPCN6 (for Topology-related Design Variable, Par_{LDN}=2, Par_{HDN}=2)

	Topology-related Design Variables	
	Par_{LDN}	Par_{HDN}
Designation1 Corresponding to Minimum Weight	2	2
Designation2 Corresponding to Maximum Displacement	2	2
Designation3 Corresponding to Maximum Force	2	2

	Size-related Design Variables												
	1	2	3	4	5	6	7	8	9	10	11	12	13
Designation1 Corresponding to Minimum Weight	PIPEST25	PIPST19	PIPEST13	PIPST19									
Designation2 Corresponding to Maximum Displacement	PIPST89	PIPEST19	PIPEST13	PIPDEST127									
Designation3 Corresponding to Maximum Force	PIPEST19	PIPDEST152	PIPDEST51	PIPDEST51									

	Entire Weight (kN)	Elem. Force (kN)	Node Disp. (mm)	Maximum Load Step
Designation1 Corresponding to Minimum Weight	6.3865	1304.2828	1.2521	3
Designation2 Corresponding to Maximum Displacement	76.7392	198652.1573	25.1757	5
Designation3 Corresponding to Maximum Force	72.3115	653761.0440	15.0639	6

to a reduce in the entire weight of dome structure to its lowest value 6.3865 kN (see Table 7). But, it is also noted that the weight reduction causes to decrease in load-carrying capacity of dome structure. However, when the designation corresponding to the lowest entire weight value 6.3865 kN is considered, it is seen that the load-carrying capacity, 1304.2828 kN is the lowest compared to the other extreme designations' (see Tables 7-9).

It is clear that an increase in the entire weight of dome structure leads to an elevation in values of its node displacement and load-carrying capacity of its members. Because, the load step numbers that determine load-displacement increments in the nonlinear structural analyses are increased.

Table 8 Values of size, shape-related design variable corresponding to designations with minimum weight, maximum displacement and maximum force obtained by use sphere-shaped geometrical configuration2 and GPCN8 (for Topology-related Design Variable, Par_{LDN}=5, Par_{HDN}=5)

	Topology-related Design Variables	
	Par_{LDN}	Par_{HDN}
Designation1 Corresponding to Minimum Weight	5	5
Designation2 Corresponding to Maximum Displacement	5	5
Designation3 Corresponding to Maximum Force	5	5

	Size-related Design Variables												
	1	2	3	4	5	6	7	8	9	10	11	12	13
Designation1 Corresponding to Minimum Weight	PIPST89	PIPEST38	PIPST19	PIPEST38	PIPST32	PIPEST64	PIPST32	PIPEST38	PIPST127	PIPEST19	PIPEST25	PIPDEST51	PIPEST76
Designation2 Corresponding to Maximum Displacement	PIPEST305	PIPEST19	PIPST102	PIPDEST127	PIPDEST76	PIPEST254	PIPEST254	PIPEST305	PIPEST13	PIPDEST51	PIPEST51	PIPST25	PIPST25
Designation3 Corresponding to Maximum Force	PIPST203	PIPEST32	PIPST32	PIPEST25	PIPDEST203	PIPEST305	PIPDEST152	PIPST89	PIPST32	PIPST76	PIPDEST102	PIPST305	PIPEST203

	Entire Weight (kN)	Elem. Force (kN)	Node Disp. (mm)	Maximum Load Step
Designation1 Corresponding to Minimum Weight	73.4320	1585.2410	0.4129	4
Designation2 Corresponding to Maximum Displacement	357.1588	38846.2703	27.9652	6
Designation3 Corresponding to Maximum Force	436.0169	476752.6054	13.4257	6

However, this fact is conflicted with the tabulated results of extreme optimal designations in Table 7. Considering Table 7, an increase in entire weight of dome structure from 72.3115 kN to 76.7392 kN causes a decrease in load-carrying capacity from 653761.0440 kN to 198652.1573 kN, but an increase in the node displacement values from 15.0639 mm to 25.1757 mm. Similarly, an increase in entire weight from 357.1588 kN and 294.8972 kN to 436.0169 kN and 350.1250 kN causes a decrease in node displacement value from 27.9652 mm and 27.5528 mm to 13.4257 mm and 19.7811 mm. Therefore, solely usage of a single objective function (for example entire weight of

Table 9 Values of size, shape-related design variable corresponding to designations with minimum weight, maximum displacement and maximum force obtained by use sphere-shaped geometrical configuration2 and GPCN8 (for Varying Topology-related Design Variable)

	Topology-related Design Variables	
	Par_{LDN}	Par_{HDN}
Designation1 Corresponding to Minimum Weight	2	2
Designation2 Corresponding to Maximum Displacement	3	3
Designation3 Corresponding to Maximum Force	2	5

	Size-related Design Variables												
	1	2	3	4	5	6	7	8	9	10	11	12	13
Designation1 Corresponding to Minimum Weight	PIPEST19	PIPEST32	PIPST51	PIPST32									
Designation2 Corresponding to Maximum Displacement	PIPEST152	PIPDEST76	PIPDEST102	PIPDEST64	PIPST38	PIPDEST152	PIPEST305						
Designation3 Corresponding to Maximum Force	PIPDEST76	PIPDEST152	PIPDEST64	PIPEST305									

	Entire Weight (kN)	Elem. Force (kN)	Node Disp. (mm)	Maximum Load Step
Designation1 Corresponding to Minimum Weight	11.4337	6556.0100	2.0420	4
Designation2 Corresponding to Maximum Displacement	294.8972	350569.0328	27.5528	6
Designation3 Corresponding to Maximum Force	350.1250	1562597.4696	19.7811	7

dome structure) for design optimization of geometrically nonlinear dome structure is not appropriate for accurately assessment of an optimal design. In this regard, the usage of multi-objective optimization approach increases the correctness degree in the assessment of optimality quality.

7. Conclusions

In this study, the size and topology of dome structures, geometrical configurations of which are automatically generated, is optimized by use of an optimization tool named NSGA II coded in

MATLAB. Three objective function values are computed in case of termination during executing computing procedure of nonlinear structural analysis method once the member strengths or node displacements does not satisfy the design requirements of API RP2A-LRFD. Therefore, it does not require any penalization process. For this purpose, three distinct sphere-shaped geometrical configurations that are generated by an automatic dome generator tool are employed. Total eight genetic operator parameter sets are utilized in order to determine the most appropriate parameter set leading to an increase in the computing performance of NSGA II algorithm.

The proposed optimization procedure is performed to optimize the design of a dome structure. It is demonstrated that the optimality quality of designations are increased when the dome structure is designed thereby utilizing longitudinal, horizontal and diagonal members along with a genetic operator parameter set with lower crossover and mutation rates. Furthermore, it is also shown that the usage of multiple objectives at same time increases the accuracy in the evaluation of optimality degree of designations.

Consequently, the proposed design optimization approach is recommended to optimize the design of geometrically nonlinear dome structures. As a next study, the shape of dome structure will be also included into the size and topology optimization procedure. Also, different multi-objective optimization algorithms will be proposed to compare their computing performance with NSGA II algorithm.

References

Carbas, S. and Saka, M.P. (2011), "Optimum topology design of various geometrically nonlinear latticed domes using improved harmony search method", *Struct. Multidiscip. O.*, **1**, 1-23.

Cardoso, J.B. and Arora, J.S. (1988), "Variational method for design sensitivity analysis in nonlinear structural mehanics", *AIAA J.*, **26**, 5-22.

Choi, K.K. and Santos, J.L.T. (1987), "Design sensitivity analysis of nonlinear structural systems, Part I: theory" *Int. J. Numer. Meth. Eng.*, **24**, 2039-2055.

Deb, K. and Goel, T. (2001a), "Controlled elitist non-dominated sorting genetic algorithms for better convergence", *Lecture Notes in Computer Science*, **1993**, 67-81.

Deb, K. (2001b), *Multi-Objective Optimization using Evolutionary Algorithms*, John Wiley & Sons.

Deb, K., Agrawal, S., Pratap, A. and Meyarivan, T. (2002), "A fast and elitist multiobjective genetic algorithm:NSGA-II", *IEEE T. Evol. Comput.*, **6**(2), 182-197.

Fonseca, C.M. and Fleming, F.J. (1993), "Genetic algorithms for multiobjective optimization: formulation, discussion and generalization", *Proceedings of the Fifth International Conference on Genetic Algorithms*, 416-423.

Forde, B.W.R. and Stiemer, S.F. (1987), "Improved arc-length orthogonality methods for nonlinear finite element analysis", *Comput. Struct.*, **27**, 625-630.

Hasancebi, O., Carbas, S., Dogan, E., Erdal, F. and Saka, M.P. (2009), "Performance evaluation of metaheuristic search techniques in the optimum design of real size pin jointed structures", *Comput. Struct.*, **87**, 284-302.

Horn, J.N., Nafpliotis, A.L. and Goldberg, D.E. (1994), "A niched pareto genetic algorithm for multiobjective optimization", *Proceedings of the First IEEE Conference on Evolutionary Computation,IEEE World Congress on Computational Intelligence*, 82-87.

Hrinda, G.A. and Nguyen, D.T. (2008), "Optimization of stability-constrained geometrically nonlinear shallow trusses using an arc length sparse method with a strain energy density approach", *Finite Elem. Analy. Des.*, **44**, 933-950.

http://iridia.ulb.ac.be/~manuel/hypervolume.

Kamat, M.P., Khot, N.S. and Venkayya, V.B. (1984), "Optimization of shallow trusses against limit point instability", *AIAA J.*, **22**, 403-408.

Kannan, S., Baskar, S., MacCalley, J.D. and Murugan, P. (2009), "Application of NSGAII algorithm to generation expansion palnning", *IEEE T. Power Syst.,* **24**(1), 454-461.

Kaveh, A. and Talatahari, S. (2010), "Optimal design of schwedler and ribbed domes via hybrid big bang-big crunch algorithm", *J. Constr. Steel Res.*, **66**(3), 412-419.

Kaveh, A. and Talatahari, S. (2011), "Geometry and topology optimization of geodesic domes using charged system search", *Struct. Multidiscip. O.*, **43**(2), 215-229.

Khot, N.S. and Kamat, M.P. (1985), "Minimum weight design of truss structures with geometric nonlinear behavior", *AIAA J.*, **23**, 139-144.

Levy, R. and Perng, H.S. (1988), "Optimization for nonlinear stability", *Comput. Struct.*, **30**, 529-535.

Levy, R. (1994a), "Optimization for buckling with exact geometries", *Comput. Struct.*, **53**, 1139-1144.

Levy, R. (1994b), "Optimal design of trusses for overall stability", *Comput. Struct.*, **53**(5), 1133-1138.

Ohsaki, M. (2001), "Sensitivity analysis and optimization corresponding to a degenerate critical point", *Int. J. Solid Struct.*, **38**, 4955-4967.

Ohsaki, M. (2005), "Design sensitivity analysis and optimization for nonlinear buckling of finite-dimensional elastic conservative structures", *Comput. Meth. Appl. Mech. Eng.*, **194**, 3331-3358.

Ohsaki, H.M. and Ikeda, K. (2006), "Imperfection sensitivity analysis of hill-top branching with many symmetric bifurcation points", *Int. J. Solid Struct.*, **43**(16), 4704-4719.

Saka, M.P. and Kameshki, E.S. (1998), "Optimum design of nonlinear elastic framed domes", *Adv. Eng. Software*, **29**(7-9), 519-528.

Saka, M.P. (2007a), "Optimum geometry design of geodesic domes using harmony search algorithm", *Adv. Struct. Eng.*, **10**, 595-606.

Saka, M.P. (2007b), "Optimum topological design of geometrically nonlinear single layer latticed domes using coupled genetic algorithm", *Comput. Struct.*, **85**, 1635-1646.

Santos, J.L.T. and Choi, K.K. (1988), "Sizing design sensitivity analysis of nonlinear structural systems, Part II", *Int. J. Numer. Meth. Eng.*, **26**, 2039-2055.

Schaffer, J.D. (1984), "Multiple objective optimization with vector evaluated genetic algorithms", Ph.D. Thesis, Vanderbilt University.

Sedaghati, R. and Tabarrok, B. (2000), "Optimum design of truss structures undergoing large deflections subject to a system stability constraint", *Int. J. Numer. Meth. Eng.*, **48**(3), 421-434.

Sepehri, A., Daneshmand, F. and Jafarpur, K. (2012), "A modified particle swarm approach for Multiobjective optimization of laminated composite structures", *Struct. Eng. Mech.*, **42**(3), 335-352.

Srinivas, N. and Deb, K. (1995), "Multiobjective optimization using nondominated sorting in genetic algorithms", *Evol. Comput.*, **2**(3), 221-248.

Sunar, M. and Kahraman, R. (2001), "A comparative study of multiobjective optimization methods in structural design", *Turkish J. Eng. Environ. Sci.*, **25**(2), 69-78.

Talaslioglu, T. (2011), "Multiobjective design optimization of grillage systems according to LRFD-AISC", *Adv. Civil Eng.*, Hindawi Press.

Tanaka, M. and Tanino, T. (1992), "Global optimization by the genetic algorithm in a multiobjective decision support system", *Proceedings of the 10th International Conference on MultipleCriteria Decision Making*, 261–270.

Zhou, A., Qu, B.Y., Li, H., Zhao, S.Z. and Suganthan, P.N. (2011), *Multiobjective Evolutionary Algorithms: A Survey of the State of Art*, Swarm and Evolutionary Computation, **1**, 32-49.

Appendix

Member strength related design requirements based on provisions of API RP2A-LRFD specification

(See Section D, named Cylindrical Member Design, in API RP2A-LRFD Specification)

$$Unity_{Axial} = \begin{cases} \dfrac{f_t}{(\phi_t * F_y)} \\ \dfrac{f_c}{(\phi_c * F_{cn})} \end{cases} \tag{20}$$

Where

$$F_{cn} = \begin{cases} (1.0 - 0.25 * \lambda^2) * F_y, & \lambda < \sqrt{2} \\ \dfrac{1}{\lambda^2} * F_y, & \lambda \geq \sqrt{2} \end{cases} \tag{21}$$

$$\lambda = \frac{K * L}{\pi * r}\left(\frac{F_y}{E}\right)^{0.5} \tag{22}$$

$$F_y = \min(F_{xe} \text{ and } F_{xc}) \tag{23}$$

$$F_{xe} = 2 * C_x * E * (t/D) \quad (C_x = 0.3) \tag{24}$$

$$F_{xc} = \begin{cases} F_y & \dfrac{D}{t} \leq 60 \\ (1.64 - 0.23 * (D/t)^{1/4}) * F_y \ldots & \dfrac{D}{t} > 60 \end{cases} \tag{25}$$

$$Unity_{Bending} = \begin{cases} \dfrac{f_{by}}{(\phi_b * F_{bn})} \\ \dfrac{f_{bz}}{(\phi_b * F_{bn})} \end{cases} \tag{26}$$

$$Unity_{CombinedBending} = \frac{(f_{by}^2 + f_{bz}^2)^{0.5}}{(\phi_b * F_{bn})} \tag{27}$$

Where

$$F_{bn} = \begin{cases} (Z/S) * F_y & (D/t) \leq (1500/F_y) \\ (1.13 - 2.58 * F_y * D/(E * t)) * ((Z/S) * F_y) & (1500/F_y) < (D/t) \leq 3000 \\ (0.94 - 0.76 * ((F_y * D)/(E * t))) * ((Z/S) * F_y & (3000/F_y) < (D/t) \leq 3000 \end{cases} \tag{28}$$

$$Unity_{Shear} = \frac{((2 * V)/A)}{(\phi_v * (F_y/\sqrt{3}))} \tag{29}$$

$$Unity_{Torsion} = \frac{((M_{vt} * D)/(2 * I_p))}{(\phi_v * (F_y/\sqrt{3}))} \tag{30}$$

$$Unity_{AxialCompr\&BendingBuck} = \frac{f_c}{(\phi_c*F_{cn})} + \frac{1}{(\phi_b*F_{bn})}*\left(\left(\frac{C_{my}*f_{by}}{1-\frac{f_e}{(\phi_c*F_{ey})}}\right)^2 + \left(\frac{C_{my}*f_{bz}}{1-\frac{f_e}{(\phi_c*F_{ez})}}\right)^2\right) \tag{31}$$

Where

$$F_{ey} = (F_y/\lambda_y^2) \tag{32}$$

$$F_{ez} = (F_y/\lambda_z^2) \tag{33}$$

$$Unity_{AxialCompr\&BendingYield} = \begin{cases} 1-\cos\left(\frac{\pi*f_c}{2*\phi_c*F_{xc}}\right) + \frac{((f_{by})^2+(f_{bz})^2)^{0.5}}{\phi_b*F_{bn}} \\ \frac{f_c}{\phi_c*F_{xc}} \end{cases} \tag{34}$$

Nonations

Member-related Design Constraints

- f_c : Axial Compressive Stress due to Factored Loads
- F_{bn} : Nominal Bending Strength
- f_t : Axial Tensile Stress due to Factored Loads
- f_b : Bending Strength due to factored Loads
- F_y : Nominal Yield Strength
- S : Elastic Section Modulus
- Φ_{cn} : Nominal Axial Compressive Strength
- Φ_b : Resistance Factor for Bending Strength (0.95)
- Φ_t : Resistance Factor for Axial Tensile Strength (0.95)
- Z : Plastic Section Modulus
- Φ_c : Resistance Factor for Axial Compressive Strength (0.85)
- f_v : Maximum Shear Stress due to Factored Loads
- λ : Column Slenderness Parameter
- V : Beam Shear due to Factored Loads
- E : Young's Modulus of Elasticity
- A : Cross-sectional Area
- K : Effective Length Factor
- Φ_v : Resistance Factor for Beam Shear Strength (0.95)
- L : Unbraced Length
- f_v : Maximum Shear Stress due to Factored Loads
- r : Radius of Gyration
- M_{vt} : Torsional Moment due to Factored Loads
- F_{xe} : Nominal Elastic Local Buckling Strength
- I_p : Polar Moment of Inertia
- F_{xc} : Nominal In-elastic Local Buckling Strength
- F_{ey} : Euler Buckling Strengths Corresponding to Element y Axes
- C_x : Critical Elastic Buckling Coefficient
- F_{ez} : Euler Buckling Strengths Corresponding to Element z Axes
- D : Outside Diameter
- λ_y : Column Slenderness Parameter for Element y Axes
- t : Wall Thickness
- λ_z : Column Slenderness Parameter for Element z Axes